INSTITUTE OF PHYSICS PUBLISHING PHYSIOLOGICAL MEASUREMENT

Physiol. Meas. **24** (2003) 251–260 PII: S0967-3334(03)56535-2

In vivo electrical conductivity of hepatic tumours

Dieter Haemmerich[1,4], S T Staelin[1], J Z Tsai[2], S Tungjitkusolmun[3], D M Mahvi[1] and J G Webster[4]

[1] Department of Surgery, University of Wisconsin-Madison, 600 Highland Avenue, WI 53792, USA
[2] Department of Electrical and Computer Engineering, University of Wisconsin-Madison, 1550 Engineering Drive, Madison, WI 53706, USA
[3] Department of Electronics Engineering, King Mongkut's Institute of Technology Ladkrabang, Chalongkrung Road, Ladkrabang, Bangkok, 10520, Thailand
[4] Department of Biomedical Engineering, University of Wisconsin-Madison, 1550 Engineering Drive, Madison, WI 53706, USA

E-mail: haemmeri@surgery.wisc.edu

Received 21 November 2002, in final form 12 January 2003
Published 7 February 2003
Online at stacks.iop.org/PM/24/251

Abstract

Knowledge of electrical tissue conductivity is necessary to determine deposition of electromagnetic energy and can further be used to diagnostically differentiate between normal and neoplastic tissue. We measured 17 rats with a total of 24 tumours of the K12/TRb rat colon cancer cell line. In each animal we measured *in vivo* hepatic tumour and normal tissue conductivity at seven frequencies from 10 Hz to 1 MHz, at different tumour stages between 6 and 12 weeks after induction. Conductivity of normal liver tissue was 1.26 ± 0.15 mS cm^{-1} at 10 Hz, and 4.61 ± 0.42 mS cm^{-1} at 1 MHz. Conductivity of tumour was 2.69 ± 0.91 mS cm^{-1} at 10 Hz, and 5.23 ± 0.82 mS cm^{-1} at 1 MHz. Conductivity was significantly different between normal and tumour tissue ($p < 0.05$). We determined the percentage of necrosis and fibrosis at the measurement site. We fitted the conductivity data to the Cole–Cole model. For the tumour data we determined Spearman's correlation coefficients between the Cole–Cole parameters and age, necrosis, fibrosis and tumour volume and found significant correlation between necrosis and the Cole–Cole parameters ($p < 0.05$). We conclude that necrosis within the tumour and the associated membrane breakdown is likely responsible for the observed change in conductivity.

Keywords: tumour conductivity, tissue conductivity, electrical properties

1. Introduction

The knowledge of conductivity of neoplastic tissue compared to normal liver parenchyma can be used for detection of tumour via bioimpedance measurement. As early as 1926 Fricke and Morse (1926) reported differences in permittivity between normal and malignant breast tissue and suggested that reliable diagnosis could be based on such differences. Radio-frequency ablation has become an important means of treatment for nonresectable liver tumours by producing localized hyperthermia and destroying the cancerous tissue. Since the distribution of absorbed electromagnetic energy depends on the ratios of electrical conductivity between the different tissues involved, quantification of conductivity of normal and malignant tissue is necessary to accurately determine energy deposition.

There are only a few studies on electrical properties of neoplastic tissue at audio and radio frequencies, especially *in vivo*. It has been shown that conductivity changes significantly after tissue has been removed from the body, and that accurate measurements require an *in vivo* setting (Haemmerich *et al* 2002). Smith *et al* (1986) report *in vitro* electrical properties of liver carcinoma from 1 kHz to 13 MHz. Morimoto *et al* (1993) report results of human *in vivo* measurements for breast and pulmonary carcinomas, which are to our knowledge the only *in vivo* results for electrical properties of tumour in the radio-frequency range. Swarup *et al* (1991) measured tumours *in vitro* at different stages from 10 kHz to 100 MHz. McRae and Esrick (1992) report change of electrical properties of tumour *in vitro* during hyperthermia from 100 Hz to 40 MHz. Some investigators acquired measurements at high radio frequencies. Lu *et al* (1992) measured brain tumour *in vitro* at frequencies of 5 to 500 MHz. Peloso *et al* (1984) measured rat tumour *in vitro* at 1 MHz to 1 GHz and found no significant difference to normal tissue. Others report results in the microwave frequency range where the differences between normal and tumour tissue stem primarily from differences in water content (Schepps and Foster 1980, Zywietz and Knoechel 1986, Burdette *et al* 1977). There are no known reports on *in vivo* measurements of electrical conductivity of hepatic tumours at audio and radio frequencies.

2. Materials and methods

2.1. Tumour model

We obtained pre-approval for all animal experiments from the Institutional Animal Care and Use Committee, University of Wisconsin, Madison. We used the K12/TRb colon cancer line for inducing tumours in the BD-IX strain of brown rat. The K12/TRb cell line was chosen because it has similar histological characteristics to those of human colon cancer. The tumour cells were harvested in standard cell culture using Dulbecco's Modified Eagle Medium (DMEM) at 37 °C, with 5% CO_2. After the cells were grown, they were suspended in phosphate-buffered saline (PBS). A total of 40 BD-IX rats were injected with tumour cells. Before injection, the animals were anesthetized by intraperitoneal injection of ketamine and xylazine.

The first set of 20 rats received intrahepatic injections, which were performed through small lesions, using sterile methods. The left lobe of the liver was injected with 50 μl of tumour cell suspension containing $\sim 10^6$ tumour cells. Fourteen of the 20 injected animals survived and developed a total of 17 tumours of sufficient size for conductivity measurement. The second set of 20 received intrasplenic injections through small incisions, using sterile methods. The rats' spleens were injected with 500 μl of tumour cell suspension containing $\sim 8 \times 10^6$ tumour cells. This method resulted in variable degrees of liver metastases. Three of the

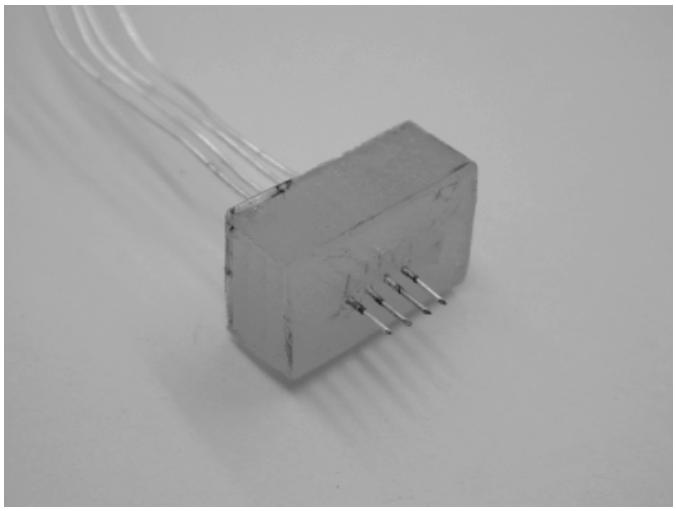

Figure 1. Plunge probe used for conductivity measurement.

animals receiving intrasplenic injections developed tumours suitable for including them in the study, developing a total of seven tumours. The rat tumour model, where 40 rats were injected with tumour cells, resulted in a total of 17 rats carrying 24 tumours, where tumour conductivity was measured. The rats were opened after 6 weeks to start the measurement of tissue conductivity. For each rat normal liver tissue was measured as a control. Each week, up to 12 weeks after injection, one to three rats were randomly chosen so that data for three to five tumours could be acquired at each time point. After measurement, the rats were sacrificed, and the liver was excised for histologic processing.

2.2. Tissue processing

After excision of the liver, the tumours were measured with a caliper, and tumour volume was estimated. Then the tumours were sectioned and the location of the conductivity probe was determined. Tumour sections were stained in standard H&E stain. The tumour sections were examined at 10× magnification in the region where the conductivity probe was placed. This region was easily identifiable as an area of haemorrhage. All tissue within the field of view around the location of prior probe placement was examined, and a staff pathologist assigned percentage values for the area of necrosis and fibrosis.

2.3. Measurement system

We used the four-terminal measurement method which minimizes the effects of polarization impedance and has been widely used for conductivity measurements in mammalian tissue (Rush *et al* 1963, Steendijk *et al* 1993, Bragos *et al* 1996). We used a four-electrode silver 0.38 mm diameter plunge probe with electrode spacing of 1.5 mm and depth of 6 mm (see figure 1). The proximal 2 mm of the probe was insulated to reduce errors caused by fluid buildup on the probe surface. Before conducting the measurements, the Ag electrodes were covered with AgCl by electrolytic deposition to reduce artefacts. We calibrated the setup with 0.9% saline solution at 25 °C. Tsai *et al* (2000) used this measurement circuit in previous studies on heart resistivity measurements.

A HP54600B digital oscilloscope was used to measure induced current and voltage drop at the probe. The input signal was generated using a HP33120A function generator. Both the oscilloscope and the function generator feature an RS232 serial port. We used an IBM-PC compatible computer for controlling the signal generator and acquiring data from the oscilloscope. The program running on the PC for controlling the devices was written in Microsoft Visual Basic and entered the measured data together with the calculated conductivity values into a Microsoft Excel Sheet for further processing. We measured conductivity at frequencies of 10 Hz, 100 Hz, 1 kHz, 10 kHz, 100 kHz, 460 kHz and 1 MHz. The measurement at 460 kHz was carried out since this frequency is used in commercial radio-frequency ablation devices for ablation of liver tumours.

2.4. Data analysis

The conductivity data acquired from tumour and normal tissue conductivity measurements were fitted to the widely used Cole–Cole model using the least-squares error method. The Cole–Cole equation for complex conductivity is (Foster and Schwan 1989):

$$\sigma^*(\varpi) = \sigma + \mathrm{j}\omega\varepsilon = \sigma_\infty + \frac{\sigma_\mathrm{S} - \sigma_\infty}{1 + (-\mathrm{j}\omega\tau_\mathrm{C})^{(1-\alpha)}} + \mathrm{j}\omega\varepsilon_0\varepsilon_\infty. \tag{1}$$

In equation (1), σ^* is the complex conductivity, σ is the conductivity and ε is the permittivity. Since we only measured conductivity (σ), the measured data were fitted to the real part of equation (1):

$$\sigma(f) = \sigma_\infty + (\sigma_\mathrm{S} - \sigma_\infty)\frac{1 + \left(\frac{f}{f_\mathrm{C}}\right)^{1-\alpha} \sin\left(\alpha\frac{\pi}{2}\right)}{1 + \left(\frac{f}{f_\mathrm{C}}\right)^{2(1-\alpha)} + 2\left(\frac{f}{f_\mathrm{C}}\right)^{1-\alpha} \sin\left(\alpha\frac{\pi}{2}\right)}. \tag{2}$$

Four parameters were acquired for each dataset that was fit to equation (2): σ_S, σ_∞, f_C and α. Since the Cole–Cole equation is deduced from an empirical model, these parameters do not have a direct physical significance. Nevertheless, the parameter σ_S corresponds to the conductivity at low frequencies. The parameter α determines the spread of relaxation frequencies within the tissue (i.e. the higher α is, the more spread are the relaxation frequencies). The parameter σ_∞ is an estimate of conductivity at high frequencies ($\sim 10^{10}$ Hz). Since the measurement frequency range only extends up to 1 MHz, this estimate is not meaningful in our case. Similarly, the estimates for the parameters of f_C and α are only poor approximations due to the limited frequency range. Good estimates for these parameters would require an extension of the measurement range to above the relaxation frequencies to $\sim$100 MHz. The error between the Cole–Cole approximation and the data was below 5% for each of the conductivity datasets.

We conducted a Wilcoxon signed rank test to determine if there is any difference between the Cole–Cole parameters of normal tissue compared to tumour tissue. Within the data from the tumour conductivity measurements, we determined Spearman's correlation coefficients to reveal any correlation between the Cole–Cole parameters and age, necrosis, fibrosis and tumour volume.

3. Results

Figure 2 shows the interface section where normal liver tissue and tumour converge. The white line approximates the boundary between the two sections. The section with normal liver parenchyma is much more homogenous compared to the tumour region. As the tumour

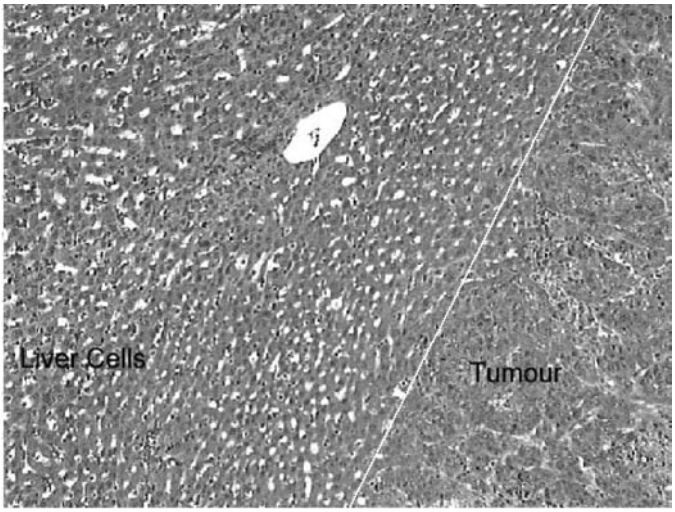

Figure 2. Interface section (10×) of liver and tumour tissue.

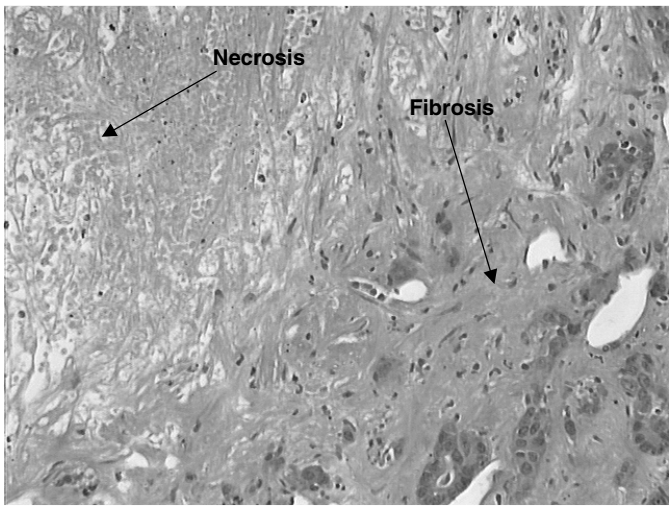

Figure 3. Tumour section (10×) with regions of necrosis and fibrosis.

grows, the connecting liver tissue gets compressed. The resulting higher density of liver cells close to the boundary can also be seen in figure 2.

Figure 3 shows tumour regions, where sections of fibrosis and necrosis can be seen. Necrosis can be identified in the images as the light sections, where no living cells can be found (only few or no cell nuclei, which appear as black dots, are visible). Fibrosis appears in the images as grey strands of tissue. Viable tumour cells appear in dark grey.

Figure 4 shows the average and standard deviation of all 24 conductivity datasets for normal liver and tumour tissues.

We conducted the Wilcoxon signed-ranks test between the Cole–Cole parameters of normal liver and tumour tissues to find the significance of difference between the parameters. The p-values resulting from this test are reported in table 1. Significant difference between

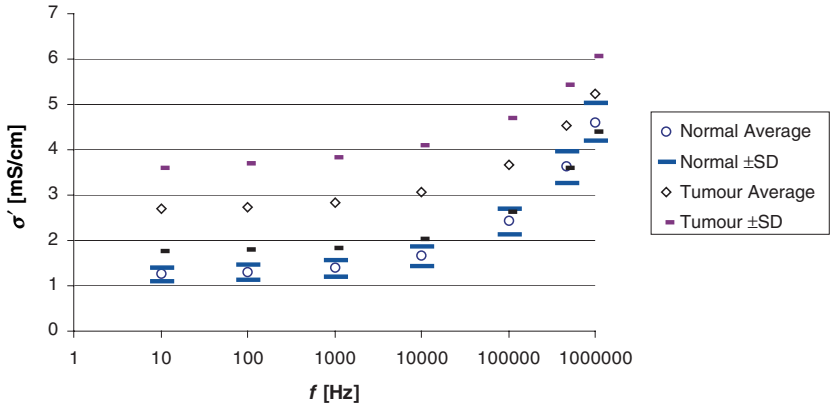

Figure 4. Mean ± SD. Electrical conductivity of tumour and normal liver tissue.

Table 1. *p*-values for Wilcoxon test.

Parameter	*p*-value
σ_S	2.29×10^{-8}
σ_∞	8.56×10^{-4}
α	0.45
f_C	0.69

Table 2. Spearman's correlation coefficients between Cole–Cole parameters (left-hand side) and tumour parameters (top). Corresponding *p*-values are in brackets. *p*-values where significance (at 5% level) is reached are underlined.

	Volume (mm^3)	Fibrosis (%)	Necrosis (%)	Total (%)	Age (days)
σ_S (mS cm^{-1})	0.50 (0.013)	0.16 (0.448)	0.61 (0.001)	0.60 (0.002)	−0.13 (0.553)
σ_∞ (mS cm^{-1})	−0.20 (0.347)	−0.39 (0.061)	−0.57 (0.004)	−0.59 (0.003)	0.64 (0.001)
α	−0.20 (0.347)	0.30 (0.157)	0.55 (0.006)	0.55 (0.005)	−0.26 (0.213)
f_C (MHz)	−0.21 (0.318)	0.45 (0.027)	0.19 (0.383)	0.28 (0.182)	−0.35 (0.097)

the means of normal and tumour tissues for parameters σ_S and σ_∞ was found at the 0.05 level. The average of parameter σ_S (conductivity at low frequencies) is 1.24 mS cm^{-1} for normal tissue and 2.61 mS cm^{-1} for tumour tissue. No significant difference between the means of normal and tumour tissue for parameters α and f_C was found.

To further investigate the underlying reasons for the difference between normal and tumour data, Spearman's correlation coefficients were determined between each of the four Cole–Cole parameters of the tumour data and tumour volume, tumour age, percentage necrosis, percentage fibrosis and percentage total (i.e. necrosis plus fibrosis). Table 2 shows the correlation coefficients and the *p*-values that are associated with the correlation coefficients. The values where significant correlation at the 0.05 level was found are underlined.

The values of the correlation coefficients, which lie between 0.5 and 0.6 (where significance was found), correspond to a moderate to strong relationship. There was significant correlation between each of the three Cole–Cole parameters σ_S, σ_∞, α and percentage necrosis. Correlation was also found between each of these three parameters and percentage total

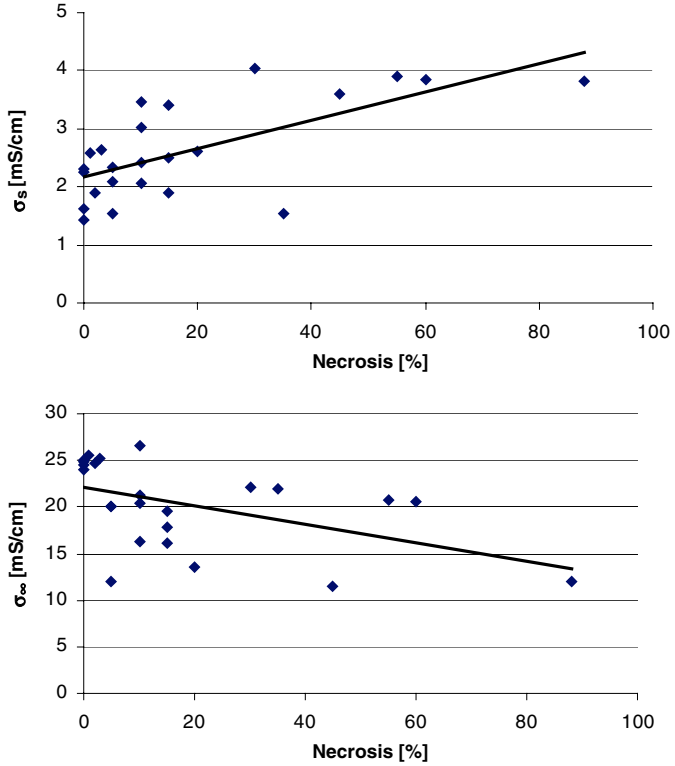

Figure 5. Scatter plots of the parameters σ_S and σ_∞ versus percentage necrosis. The line represents a first-order approximation of the data.

(necrosis plus fibrosis). The parameter f_C shows only weak correlation with percentage fibrosis, and no correlation with any of the other tumour parameters. Tumour age and tumour volume correlate to the Cole–Cole parameters σ_∞, and σ_S, respectively.

Percentage necrosis and percentage total showed the strongest relationship to the Cole–Cole parameters. In figure 5, scatter plots of each of the parameters σ_S and σ_∞ versus percentage necrosis are shown.

We conducted the Wilcoxon signed-ranks test between Cole–Cole parameters of tumours resulting from intrahepatic versus intrasplenic injections, and did not find significant difference.

4. Discussion

Tumour gets its blood supply preferentially from the neighbouring liver tissue. In the inner regions of the tumour usually relatively few blood vessels can be found. The blood delivers nutrients necessary for the cells' survival and removes waste products resulting from cellular metabolism. Due to the lack of blood vessels in the core regions of the tumour, these cells get deprived of nutrients. Furthermore, metabolic waste products accumulate resulting in a toxic environment. These two mechanisms eventually lead to cell necrosis in the inner tumour regions. Whenever cell death occurs, these cells eventually get replaced by fibroblastic tissue (scar tissue). This mechanism is also termed fibrosis.

Initially we tried to establish if there is a difference in conductivity between normal and cancerous tissue. It is apparent from figure 4, that this tumour has higher conductivity than normal liver tissue. The increase in conductivity at high frequencies, however, is not as pronounced as at low frequencies. To obtain a quantitative measure of the significance in difference, we calculated Wilcoxon's signed-ranks test for the fitted Cole–Cole parameters between normal and malignant tissue. As the results of this test in table 1 show, there is a significant difference in conductivity between normal liver tissue and tumour tissue. Since σ_S corresponds to the low-frequency conductivity, the result for σ_S confirms that tumour is significantly more conductive than normal tissue at low frequencies.

Figure 4 shows much higher variance of the conductivity data acquired from this tumour tissue as compared to normal tissue. We explain this higher variability of the data by the much higher heterogeneity of tumour cells (see figure 1). The cells vary in size and shape, and the arrangement of cells is much less uniform than in normal tissue. Therefore, large differences in conductivity can be expected between different tumours. Other variables such as tumour size, age, etc might also influence conductivity. This influence has been examined by calculating Spearman's correlation coefficients as described above. Table 2 shows the correlation coefficients with corresponding p-values. A strong correlation was found between σ_∞ and tumour age. The strongest correlation was discovered between both percentage necrosis and percentage total, and the three parameters σ_S, σ_∞ and α. Here the correlation with σ_S carries the most weight because the parameters σ_∞ and α are only poor approximations due to the limited frequency range (i.e. below 1 MHz) as discussed in section 2.4.

It has been suggested by other researchers that the differences in conductivity between cancerous and normal tissues probably stem from regions of necrosis inside the tumour (Smith *et al* 1986). It has been shown in cultures that tumours larger than 0.2 mm develop necrosis (Folkman and Hochberg 1973). In the same way it can be expected that tumour reaching a certain size develops necrosis in its inner regions *in vivo*. The range of radio frequencies falls within the region of β-dispersion. The effect of β-dispersion results from the specific dielectric properties of the cell membranes. Cell membranes are composed of lipids, and can be modelled electrically by a capacitor between intra- and extracellular electrolyte. At frequencies below the β-relaxation frequency, current is mainly confined to extracellular space (Schwan 1966). Above the region of β-dispersion, the capacitive coupling of the cell membranes allows current to pass through the membrane, which results in an increase in tissue conductivity. When cells die by the mechanism of necrosis, eventual rupture of the cell membrane results. Therefore, impedance between intra- and extracellular space for these cells decreases, since the membrane loses its insulating property. Based on the mechanism just explained, we anticipate an increase in conductivity in tissues, where necrosis is present. We expect this increase to be most prominent at frequencies below the region of β-dispersion, since the membranes have a much higher impact on tissue conductivity at these frequencies compared to high radio frequencies. This is exactly the behaviour we observe in figure 3, and is further supported by the strong positive correlation established between parameter σ_S and percentage of necrosis.

We also observed significant correlation between parameters σ_∞ and α, and percentage necrosis. However, these results should be viewed with caution, again due to the limited measurement frequency range below 1 MHz. Figure 6 shows the approximations of the Cole–Cole model to conductivity data from two different tumours. One tumour has high percentage necrosis (90%) whereas the other has low percentage necrosis (15%). The predicted frequency dependence of conductivity far above 1 MHz is likely incorrect. For example, at high frequencies above 100 MHz, the model would predict that the tumour with less percentage necrosis has higher conductivity than that with higher percentage necrosis. This prediction

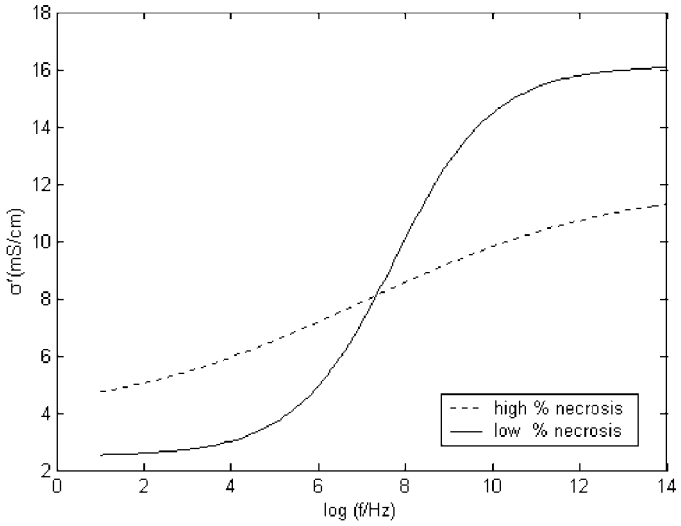

Figure 6. Cole–Cole approximation of datasets from two tumours. One tumour has high per cent necrosis (90%), and the other has low per cent necrosis (15%).

is most likely wrong. The Cole–Cole model gives incorrect estimates of conductivity at frequencies far outside the measured frequency range.

Further we found correlations between parameter σ_S and tumour volume, and between σ_∞ and tumour age. Both tumour age and tumour volume affect the amount of necrosis, and thereby impact indirectly on conductivity.

5. Conclusion

The strong correlation between necrosis and the fitted Cole–Cole parameters strongly support the hypothesis that necrosis and associated changes within tissue are responsible for the major part of the differences seen in conductivity. The differences in electrical conductivity we observed may be used to diagnose tumour by electrical impedance tomography (EIT) or other similar methods. Since the difference is largest at frequencies below 1 kHz, this frequency range would give the highest specificity in differentiating between normal and malignant tissue.

Acknowledgments

The authors wish to acknowledge Dr T F Warner for the histological analysis, and Dr G E Leverson for his help with the statistical analysis. This work has been supported by NIH grants DK58839 and HL56143.

References

Bragos R, Riu P, Warren M, Tresanchez M, Carreno A and Cinca J 1996 Changes in myocardial impedance spectrum during acute ischemia in the *in situ* pig heart *Proc. 18th Ann. Int. Conf. IEEE Eng. Med. Biol. Soc. (Amsterdam)*

Burdette E C, Seals J, Toler T C, Cain F L and Magin R L 1977 Preliminary *in vivo* probe measurements of electrical properties of tumours in mice *Int. Microwave Symp. Digest (San Diego)* pp 344–7

Folkman J and Hochberg M 1973 Self-regulation of growth in three dimensions *J. Exp. Med.* **138** 745–53

Foster K R and Schwan H P 1989 Dielectric properties of tissues and biological materials: a critical review *Crit. Rev. Biomed. Eng.* **17** 25–104

Fricke H and Morse S 1926 The electric capacity of tumours of the breast *J. Cancer Res.* **10** 340–76

Haemmerich D, Ozkan O, Tsai J Z, Staelin S T, Tungjitkusolmun S, Mahvi D M and Webster J G 2002 Changes of electrical resistivity of swine liver after occlusion and postmortem *Med. Biol. Eng. Comput.* **48** 29–33

Lu Y, Li B and Yu J 1992 Dielectric properties of human glioma and surrounding tissue *Int. J. Hypertherm.* **8** 755–60

McRae D A and Esrick M A 1992 The dielectric parameters of excised EMT-6 tumours and their change during hyperthermia *Phys. Med. Biol.* **37** 2045–58

Morimoto T, Kimura S, Konishi Y, Komaki K, Uyama T and Monden Y 1993 A study of the electrical bio-impedance of tumours *J. Invest. Surg.* **6** 25–32

Peloso R, Tuma D T and Rakesh R K 1984 Dielectric properties of solid tumours during normothermia and hyperthermia *IEEE Trans. Biomed. Eng.* **31** 725–8

Rush S, Abildskov J A and McFee R 1963 Resistivity of body tissues at low frequencies *Circ. Res.* **12** 40–50

Schepps J L and Foster K R 1980 The UHF and microwave dielectric properties of normal and tumour tissues: variation in dielectric properties with tissue water content *Phys. Med. Biol.* **25** 1149–59

Schwan H P 1966 Electrical properties of tissue and cell suspensions *Adv. Biol. Med. Phys.* **5** 147–209

Smith S R, Foster K R and Wolf G L 1986 Dielectric properties of VX-2 carcinoma versus normal liver tissue *IEEE Trans. Biomed. Eng.* **33** 522–4

Steendijk P, Mur G, Van der Velde E T and Baan J 1993 The four-electrode resistivity technique in anisotropic media: theoretical analysis and application on myocardial tissue *in vivo IEEE Trans. Biomed. Eng.* **40** 138–48

Swarup A, Stuchly S S and Surowiec A 1991 Dielectric properties of mouse MCA1 fibrosarcoma at different stages of development *Bioelectromagnetics* **12** 1–8

Tsai J Z, Cao H, Tungjitkusolmun S, Woo E J, Vorperian V R and Webster J G 2000 Dependence of apparent resistance of four-electrode probes on insertion depth *IEEE Trans. Biomed. Eng.* **47** 41–8

Zywietz F and Knoechel R 1986 Dielectric properties of Co-χ-irradiated and microwave-heated rat tumour and skin measured *in vivo* between 0.2 and 2.4 GHz *Phys. Med. Biol.* **31** 1021–9